Nesfatin-1 in Human and Murine Cardiomyocytes: Synthesis, Secretion, and Mobilization of GLUT-4

Sandra Feijóo-Bandín, Diego Rodríguez-Penas, Vanessa García-Rúa, Ana Mosquera-Leal, Manuel Francisco Otero, Eva Pereira, José Rubio, Isabel Martínez, Luisa María Seoane, Oreste Gualillo, Manuel Calaza, Tomás García-Caballero, Manuel Portolés, Esther Roselló-Lletí, Carlos Diéguez, Miguel Rivera, José Ramón González-Juanatey, and Francisca Lago

Cellular and Molecular Cardiology Research Unit and Department of Cardiology (S.F.-B., D.R.-P., V.G.-R., A.M.-L., M.F.O., E.P., J.R., J.R.G.-J., F.L.), Biostatistical Research Unit (I.M.), Endocrine Pathophysiology Research Group (L.M.S.), Neuroendocrine Interactions in Rheumatic Disease Laboratory (O.G.), Rheumatology Laboratory (M.C.), Department of Pathology (T.G.-C.), and Department of Physiology (C.D.), the Institute of Biomedical Research and University Clinical Hospital, 15706 Santiago de Compostela, Spain; and La Fe University Hospital (M.P., E.R.-L., M.R.), 46026 Valencia, Spain

Nesfatin-1, a satiety-inducing peptide identified in hypothalamic regions that regulate energy balance, is an integral regulator of energy homeostasis and a putative glucose-dependent insulin coadjuvant. We investigated its production by human cardiomyocytes and its effects on glucose uptake, in the main cardiac glucose transporter GLUT-4 and in intracellular signaling. Quantitative RT-PCR, Western blots, confocal immunofluorescence microscopy, and ELISA of human and murine cardiomyocytes and/or cardiac tissue showed that cardiomyocytes can synthesize and secrete nesfatin-1. Confocal microscopy of cultured cardiomyocytes after GLUT-4 labeling showed that nesfatin-1 mobilizes this glucose transporter to cell peripherals. The rate of 2-deoxy-D-[^{3}H]glucose incorporation demonstrated that nesfatin-1 induces glucose uptake by HL-1 cells and cultured cardiomyocytes. Nesfatin-1 induced dose- and time-dependent increases in the phosphorylation of ERK1/2, AKT, and AS160. In murine and human cardiac tissue, nesfatin-1 levels varied with diet and coronary health. In conclusion, human and murine cardiomyocytes can synthesize and secrete nesfatin-1, which is able to induce glucose uptake and the mobilization of the glucose transporter GLUT-4 in these cells. Nesfatin-1 cardiac levels are regulated by diet and coronary health. (*Endocrinology* 154: 4757–4767, 2013)

Nesfatin-1 is an 82–amino acid peptide derived from nucleobindin 2 (NUCB2) through processing by prohormone convertases, the enzymes that process proinsulin (1). First found in hypothalamic regions that regulate energy balance (1), it appears to act there (2) as an integral regulator of energy homeostasis, circadian feeding rhythm, and related endocrine functions (3, 4). It also circulates in the bloodstream, plasma levels depending on nutritional state and other metabolic circumstances (5–9). It reduces food and water intake and body weight gain in rodents (10–15), increases spontaneous physical activity and whole-body fat oxidation (13), and raises body temperature (14). These multiple metabolic effects and the reported association between plasma glucose and nesfatin-1 levels in rats and patients with type 2 diabetes (5, 8, 16) suggest that it is a glucose-dependent coadjuvant of insulin (13, 17–20), whereas its dependence on the metabolic state has suggested that plasma nesfatin-1 levels may be regulated by sustained changes in adipose tissue mass and/or inflammatory status (6, 21), two of the most important determinants of metabolic syndrome.

That peripheral sources of nesfatin-1 exist is suggested by its ability to cross the blood-brain barrier and by re-

ISSN Print 0013-7227 ISSN Online 1945-7170
Printed in U.S.A.

Received May 30, 2013. Accepted September 10, 2013.
First Published Online September 24, 2013

For News & Views see page 4443

Abbreviations: CI, coronary injury; NUCB2, nucleobindin 2; qPCR, quantitative PCR; ROI, region of interest.

ports of NUCB2 production, which is dependent on nutritional status and/or sympathetic nerve activity, by pituitary gland, gastric endocrine cells, endocrine pancreas, liver, subcutaneous and visceral adipose tissue, skeletal muscle, and testis (6, 16, 22–24). However, the only reported observations of endogenous fully processed nesfatin-1 appear to be those of Oh-I et al (1) in rat cerebrospinal fluid and Angelone et al (25) in rat cardiac extracts.

Like many other peptides that regulate and/or are regulated by feeding and metabolism, nesfatin-1 can influence cardiovascular function. In rat studies, it has induced negative inotropism and modulated lusitropism in perfused hearts (25) and increased sympathetic activity, mean arterial pressure, and heart rate (26–28). To the best of our knowledge, fully processed nesfatin-1 peptide has been detected in the human circulation using a sandwich-type ELISA (7), but it has never been identified in other human tissues. In this study, we investigated its presence in human cardiac tissue and its influence on correlated signaling proteins (ERK1/2, AKT, and AS160) and on GLUT-4 mobilization, and the effects of diet and cardiovascular disease on its levels in cardiomyocytes.

Table 1. Demographic and Clinical Characteristics of Cardiac Surgery Patients Used in the Study

	Men (n = 178)	Women (n = 90)
Demographics		
Age, mean, y	69.07	69.77
BMI, mean, kg/m^2	28.41	29.1
Normal weight (18.5–24.9 kg/m^2), n (%)	29 (16.3)	17 (18.8)
Overweight (25–29.9 kg/m^2), n (%)	95 (53.3)	34 (37.7)
Obesity (>30 kg/m^2), n (%)	49 (27.5)	37 (41.1)
HTA, n (%)	129 (72.4)	67 (74.4)
T2DM, n (%)	51 (28.6)	22 (24.4)
HLP, n (%)	93 (52.2)	52 (57.7)
Laboratory findings		
Triglycerides, mean, mg/dL	109.6	124.76
Cholesterol, mean, mg/dL	167.93	189.75
Glucose, mean, mg/dL	114.85	114.73
Drugs		
Antiplatelets, n (%)	64 (35.9)	29 (32.2)
Anticoagulants, n (%)	35 (19.6)	20 (22.2)
ACE inhibitors, n (%)	53 (29.7)	22 (24.4)
ARBs, n (%)	37 (20.7)	20 (22.2)
β-Blockers, n (%)	54 (30.3)	28 (31.1)
CCBs, n (%)	39 (21.9)	11 (12.2)
Diuretics, n (%)	95 (53.3)	41 (45.5)
OADs, n (%)	35 (19.6)	14 (15.5)
Insulin, n (%)	13 (7.3)	7 (7.7)
Cardiovascular pathologies		
Coronary injury, n (%)	96	27

Abbreviations: ACE, angiotensin-converting enzyme; ARB, angiotensin II receptor blocker; BMI, body mass index; CCB, calcium channel blocker; HLP, hyperlipidemia; HTA, arterial hypertension; OAD, oral antidiabetic drug; T2DM, type 2 diabetes mellitus.

Materials and Methods

All reagents were from Sigma-Aldrich unless otherwise stated.

Ethics

The study protocol was approved by the Galician Clinical Research Ethics Committee (2007/304). All acquisitions of human tissues were performed with informed consents and in accordance with the Declaration of Helsinki 2008 (and, when pertinent, the European Convention of Human Rights and Biomedicine [ETS 164] and the UK Human Tissue Act 2004) after approval by local medical/health research ethics committees. All animals were maintained and euthanized following protocols approved by the Animal Care Committee of the University of Santiago de Compostela in accordance with European Union Directive 2010/63.

Human tissue samples

Right atrial appendages were obtained from 268 patients undergoing valve surgery or coronary artery bypass grafting (patient characteristics in Table 1). Ventricular tissue samples from patients undergoing cardiac transplants (29) were donated by the La Fe University Hospital (Valencia, Spain). Samples of human stomachs (mucosa) were obtained from the Department of Digestive Pathology of the University Clinical Hospital (Santiago de Compostela, Spain).

Animals

Three- to four-week-old male Sprague-Dawley rats were fed for 18 weeks with the standard diet (3.85 kcal/g; 10% fat [5.6% soybean oil and 4.4% lard], 20% protein, and 70% carbohydrate [35% sucrose, 31% cornstarch, and 4% maltodextrin]; Research Diets, Inc] or the high-fat diet (4.73 kcal/g; 45% fat [5.6% soybean oil and 39.4% lard], 20% protein, and 35% carbohydrate [17% sucrose, 8% cornstarch, and 10% maltodextrin]; Research Diets, Inc.) and euthanized by decapitation. Hearts were collected and quickly frozen at −80°C. Neonatal (1- to 3-day-old) Sprague-Dawley rats were killed by cervical dislocation, and their hearts were used for establishment of primary cardiomyocyte cultures (see below).

Cell cultures

Cardiomyocytes from human atrial appendages and neonatal rat hearts and adult mouse atrial HL-1 cardiomyocytes (a gift of Dr. W. C. Claycomb of Louisiana State University Medical Center, New Orleans, Louisiana) were all cultured as described previously (30). Adult human ventricular cardiomyocytes (PromoCell GmbH) were cultured according to the supplier's instructions.

Quantitative PCR (qPCR)

Real-time RT-qPCR for NUCB2 was performed on RNA extracted with the RNeasy Total RNA Extraction Kit (QIAGEN) using Master Mix and specific primers provided by SABioscience (rat NUCB2, 145 bp, catalog no. PPR49435A, reference position 1245, GenBank NM_021663.2; rat GAPDH, 172 bp, catalog no. PPR06557A, reference position 363, Gen-

Bank NM_017008.3; human NUCB2, 126 bp, catalog no. PPH19934A, reference position 894, GenBank NM_005013.2; human GAPDH, 175 bp, catalog no. PPH00150E, reference position 1287, GenBank NM_002046.3; mouse NUCB2, 95 bp, catalog no. PPM25549A, reference position 1314, GenBank NM 016773.3; and mouse GADPH, 140 bp, catalog no. PPM02946E, reference position 309, GenBank NM 008084.2). We also performed one-step real-time RT-PCR with a Brilliant III SYBR Green QRT-PCR Master Mix Kit (Stratagene) for the following specific primers: rat CD36, 92 bp, GCGACATGATTAATGGCACA (forward) and CCTGCAAATGTCAGAGGAAA (reverse), GenBank NM 031561.2; and rat GADPH, 224 bp, GCTCATGACCACAGTCCATG (forward) and GGCATGTCAGATCCACAAC (reverse), GenBank NM 017008.4. Results were analyzed using MxPro v4 software (Stratagene).

Western blotting

Cultured cardiomyocytes (50,000 cells/cm^2) or heart tissues were lysed and subjected to SDS-PAGE/Western blotting as previously described (31), using antibodies against nesfatin-1 residues 1 to 28 (Phoenix Pharmaceuticals), ERK1/2 and phospho-ERK1/2 (Thermo Fisher Scientific), AKT and Ser-473–phosphorylated AKT (Cell Signaling Technology), AS160 and phospho-AS160 (Cell Signaling Technology), and β-actin and GAPDH (Thermo Fisher Scientific), all at 1:1000 dilutions except for AS160 (1:500 dilution).

Immunocytochemistry

With use of an Autostainer Link 48 (Dako), primary cultures of human and neonatal rat cardiomyocytes were stained with FLEX mouse anti-desmin antibodies (clone D33; Dako) and rabbit anti-nesfatin-1 antibodies (Phoenix Pharmaceuticals), both at 1:200, followed by EnVision FLEX/HRP (Dako) for detection. Normal goat serum or anti-nesfatin-1 antibody preadsorbed by nesfatin-1 peptide (Phoenix Pharmaceuticals) was used as a negative control.

Immunocytofluorescence labeling and confocal microscopy

Primary cultures of neonatal rat cardiomyocytes were deprived of serum for 12 hours before treatment with nesfatin-1 (0.01–1 μM for 10 minutes or 1 μM for 5–30 minutes) or 100 nM insulin. Cells (10,000 per ∅ 12-mm circular coverslip), and tissues were processed as described previously (31) using rabbit antibodies: anti-GLUT-4 (Abcam) at 1:100 dilution, anti-nesfatin-1 at 1:500 dilution or anti-prohormone convertase 1/3 (Abcam) at 1:100 dilution. Quantitative confocal microscopy was performed using a Leica DMIRE2 confocal microscope and software to compare GLUT-4 concentrations in the cell peripherals with those in the cytoplasm and perinuclear region, as other authors have described previously for cardiomyocytes in culture (31–34). A total of 216 cells were analyzed. For each coverslip, a minimum of 6 distinct and randomly chosen visual fields were photographed and analyzed as z-stacks using a Leica DMIRE2 confocal microscope and software. The mean intensity of Cy3 fluorescence was measured to indicate the relative expression level of the GLUT-4 glucose transporter. To measure the intensity of fluorescence in the cytoplasmic perinuclear region vs the cell peripheral cytoplasmic membrane, regions of interest (ROIs) of equal sizes were first set up manually, and then the cytoplasmic perinuclear region and the cell peripheral cytoplasmic membrane ROIs for each of several cells per field were chosen randomly and measured automatically. Cells with any of the following characteristics were excluded from analysis: atypically large or small size; perceptibly in the G_1 or later phase of the cell cycle; not in contact with at least one neighbor; and outer cytoplasmic borders not clearly distinguishable from those of their neighbors. Great care was taken to localize the ROIs well within the cell cytoplasmic perinuclear and cell peripheral areas (as indicated by the presence or absence of TO-PRO-3 fluorescence, respectively). To maximize the number of cells measured and the objectivity with which ROI localization was carried out, the process was performed twice, by 2 independent observers. Thus, more than 70 ratios were obtained for each experimental variable.

Glucose uptake experiments

Serum-deprived HL-1 cells or neonatal rat cardiomyocytes (10^4 per P24 well) were treated for 2.5 hours with nesfatin-1 (0.1–100 nM). Treatment for 1 hour with insulin (100 nM) was used as a positive control. Cells were washed twice in glucose-free HEPES-buffered saline solution at pH 7.4 (140 mM NaCl, 5 mM KCl, 2.5 mM $MgSO_4$, 1 mM $CaCl_2$, and 20 mM HEPES), and glucose uptake was determined as described previously using 2-deoxy-D-[^{3}H]glucose (PerkinElmer) (13). Nonspecific glucose uptake was determined in the presence of 10 μM cytochalasin B, and the value obtained was subtracted from all other measurements.

ELISAs

Plasma NUCB2/nesfatin-1 levels of male Sprague-Dawley rats fed for 18 weeks with the standard or high-fat diet were determined by ELISA (Phoenix Pharmaceuticals; minimum detection limit, 0.8 ng/mL; range, 0.1–1000 ng/mL; linear range, 0.8–14.1 ng/mL; intra-assay error, <10%; interassay error, <15%). NUCB2/nesfatin-1 secretion by neonatal rat cardiomyocytes was measured in the culture medium in 6-well plates in which cells had been cultured for 3 days at a density of 4.5×10^5 cells/well.

Statistical analyses

All experimental data were obtained from at least 3 independent experiments. The comparisons between groups of data were performed with the appropriate test, depending on the normality of the data. We used *t* tests with gaussian data, and Mann-Whitney *U*, Kruskal-Wallis, and Wilcoxon signed rank tests with nongaussian data. All the correlation coefficients were measured as Spearman *r*. All the analysis were done with SPSS 15.0 (IBM) or Prism 5 (GraphPad Software).

Results

NUCB2 gene expression in human and murine cardiomyocytes

qPCR showed NUCB2 mRNA in human cardiac tissue and cardiomyocyte cultures (with the highest levels, similar to those in stomach, in atrial tissue) (Figure 1A.1), in rat cardiac tissues and cardiomyocyte cultures (with

higher levels in atrial than in ventricular cells) (Figure 1B.1), and in mouse cardiac tissue and the adult mouse atrial cell line HL-1 (Figure 1C.1). That reverse transcription had proceeded properly was confirmed in each case by amplification of GAPDH, which was used to normalize all the data.

Synthesis of nesfatin-1 by human and murine cardiomyocytes

Western blots with anti-nesfatin-1 antibodies showed a 9.5-kDa band coinciding with the main band of commercial nesfatin-1 peptide in human, rat, and mouse cardiac tissue and/or cardiomyocytes (Figure 1, A.2, B.2, and C.2). In rat (Figure 2, A.1 and Cd and e) and human (Figure 2, Ba–c and Ca–c) cardiomyocytes from primary cultures, the perinuclear cytoplasm was intensely immunoreactive with anti-nesfatin-1 antibody (Figure 2A.1b). The possibility that some reactive cells were fibroblasts was ruled out by their immunoreactivity with antibodies against myosin heavy chain (data not shown) and/or desmin (Figure 2Cc) and by the use of a cytostatic agent in the culture medium to prevent fibroblast proliferation. Similarly, the cytoplasm of virtually all muscle fibers in sections of human atrial tissue was immunoreactive with anti-nesfatin-1 antibody (Figure 2Bd–f) and with anti-prohormone convertase 1/3 antibody (Figure 2Bg–i). Control stains (normal goat serum or anti-nesfatin-1 antibody preadsorbed by nesfatin-1 peptide) stained neither cultured cells (Figure 2, A.2 and Cb and e) nor cardiac tissues (data not shown).

Secretion of nesfatin-1 by primary cultures of rat cardiomyocytes

Secretion of NUCB2/nesfatin-1 into the culture medium was measured only in primary cultures of neonatal rat cardiomyocytes due to the limited cardiomyocyte populations afforded by human right atrial appendages in culture. In culture medium supporting approximately 4.5×10^5 confluent starving cells, the ELISA-measured NUCB2/nesfatin-1 concentration was 4.55 ± 0.52 ng/mg of cellular protein ($n = 21$).

Effect of nesfatin-1 treatment on GLUT-4 mobilization in cardiomyocytes

Analysis of confocal images of cultured neonatal rat cardiomyocytes with fluorescence-labeled GLUT-4 showed that 10 to 1000 nM nesfatin-1 caused significant translocation of GLUT-4 to cell peripherals, decreasing its amount in the cytoplasmic perinuclear area of the cardiomyocytes in a dose- and time-dependent fashion by a factor similar to that caused by 100 nM insulin (Figure 3).

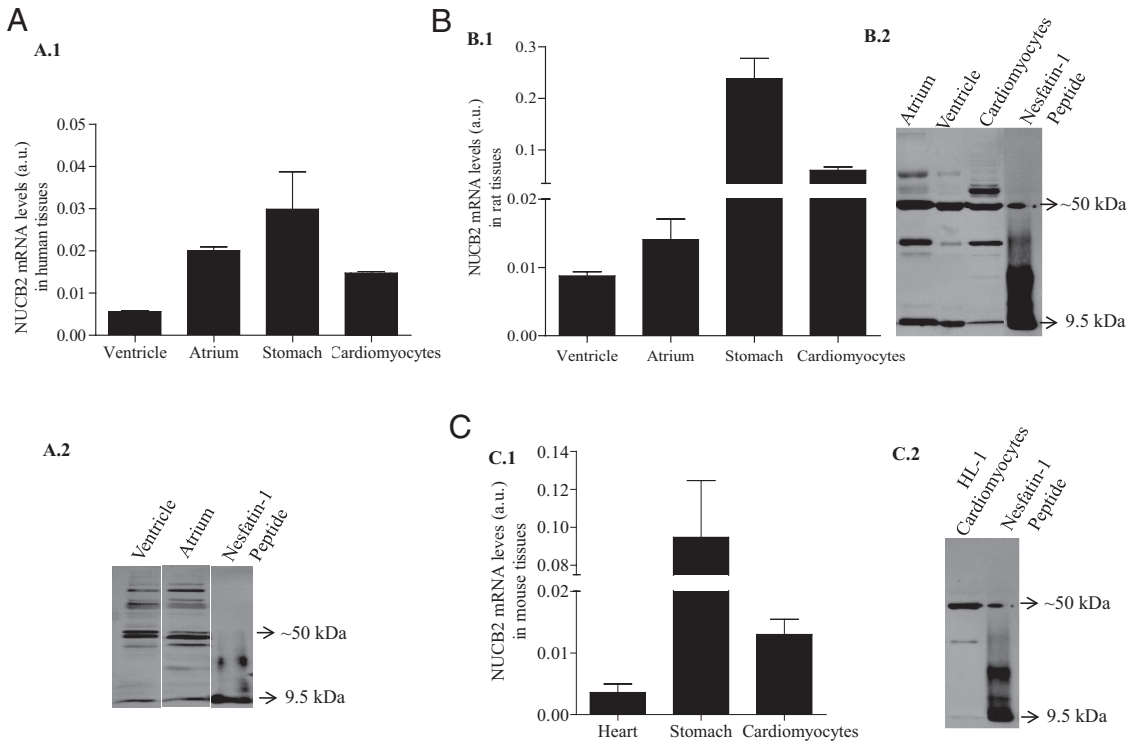

Figure 1. Results of qPCR (A.1, B.1, and C.1) and Western blots (A.2, B.2, and C.2) comparing the levels of NUCB2 mRNA and nesfatin-1 peptide (9.5-kDa band; the band at ~50 kDa corresponds to full-length NUCB2 protein), respectively, in human (A), rat (B), and mouse (C) cardiac tissues (ventricle and atrium for humans and rats and whole heart for mouse), cultured cardiomyocytes (adult human ventricular cardiomyocytes, neonatal rat cardiomyocytes, and adult mouse HL-1 cells), and stomach (mucosa) tissue. Synthetic nesfatin-1 peptide was run for comparison in Western blots. Bar graphs show means ± SEM. a.u., arbitrary units.

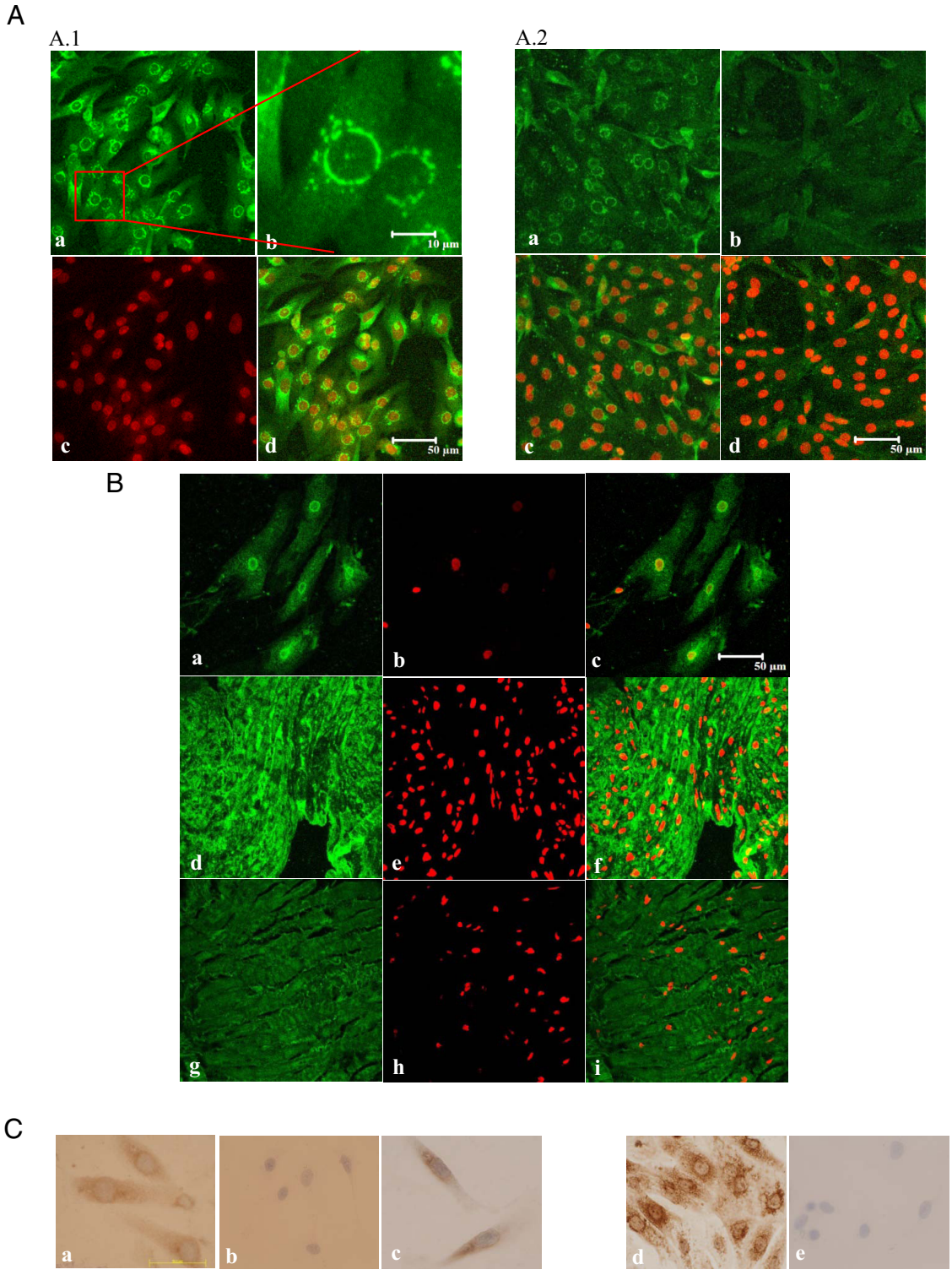

Figure 2. Nesfatin-1 in human and rat cardiomyocytes and myocardium (scale bar corresponds to 10 μm in A.1b and 50 μm elsewhere). A, Confocal photomicrographs of primary neonatal rat cardiomyocyte cultures. A.1a, Perinuclear immunofluorescent nesfatin-1. A.1b, Detail of A.1a. A.1c, TO-PRO-3 nuclear marker. A.1d, A.1a and A.1b merged. A.2a, Perinuclear immunofluorescent nesfatin-1. A.2b, No staining by anti-nesfatin-1 antibody presaturated with nesfatin-1 (negative control). A.2c, A.2a merged with the corresponding TO-PRO-3 image. A.2d, A.2b merged with the corresponding TO-PRO 3 image. B, Confocal photomicrographs of human atrial cardiomyocytes (a–c) or atrial tissue (d–i), showing immunofluorescent perinuclear nesfatin-1 (a and d) or prohormone convertase 1/3 (g), the corresponding TO-PRO 3 images (b, e, and h), and the merges of a and b, d and e, and g and h (c, f, and i). C, Immunostained nesfatin-1 in human atrial (a) and neonatal rat (d) cardiomyocytes, negative controls (b and e), and immunostained desmin in human atrial cells, confirming cardiomyocyte phenotype (c).

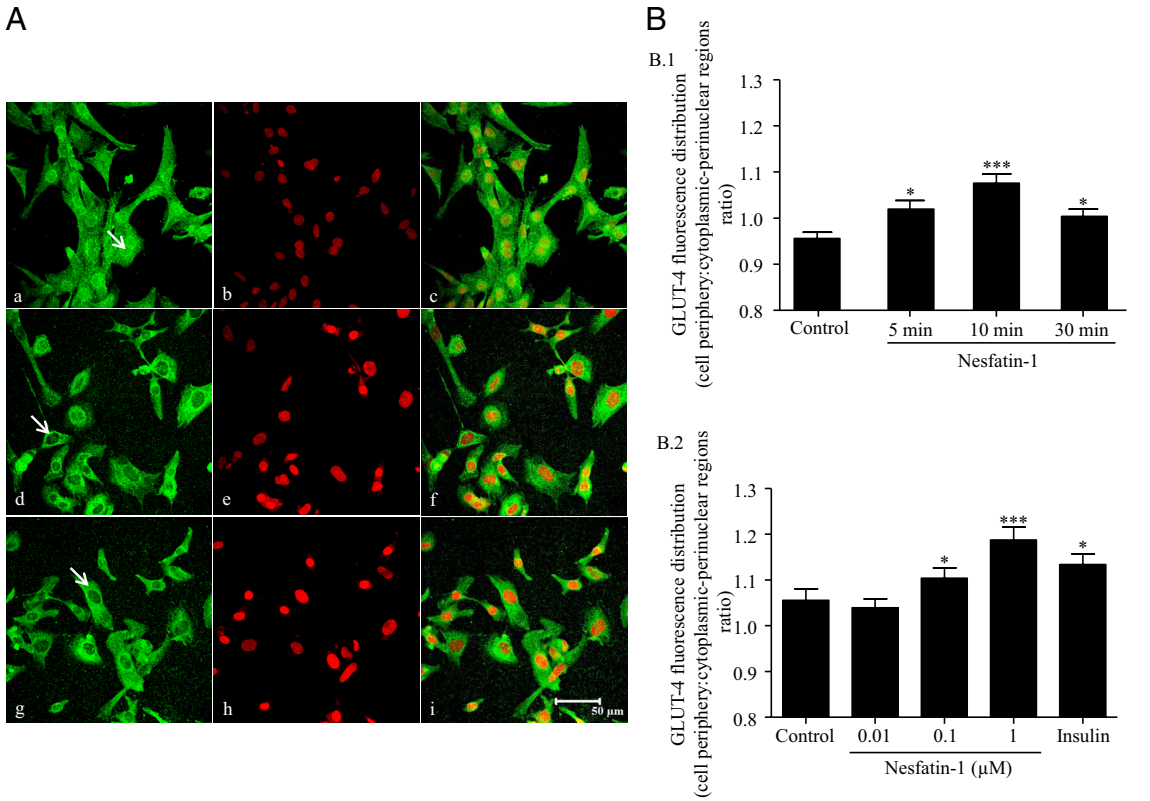

Figure 3. Translocation of glucose transporter GLUT-4 to the cell peripherals in response to nesfatin-1 treatment of neonatal rat cardiomyocytes. A, Photomicrographs of untreated cells (a–c) and cells treated with 1 μM nesfatin-1 (d–f) or 100 nM insulin (g–i), showing anti-GLUT-4 stain (a, d, and g), TO-PRO-3 nuclear marker (b, e, and h), and the corresponding merged images (c, f, and i). Note the GLUT-4 redistribution from the cytoplasmic perinuclear area (arrows) to cell peripherals in d and g. Scale bar corresponds to 50 μm. B, Ratio of GLUT-4 immunofluorescence in cell peripherals–cytoplasmic perinuclear regions in experiments showing dependence on the duration (B.1) and intensity (B.2) of exposure to nesfatin-1 (means of >70 cell peripherals–cytoplasmic perinuclear regions pairs in each of 3 replicate experiments). *, $P < .05$; ***, $P < .001$.

Effect of nesfatin-1 on glucose uptake by cardiomyocytes

Treatment with nesfatin-1 increased 2-deoxy-D-[^{3}H]glucose uptake by 12.5 ± 3.9% at 0.1 nM ($P < .05$, $n = 11$), by 11.9 ± 4% at 1 nM ($P < .05$, $n = 11$), and by 26 ± 5.4% at 100 nM ($P < .001$, $n = 11$) by HL-1 cardiomyocytes, whereas treatment with 100 nM insulin for 1 hour increased 2-deoxy-D-[^{3}H]glucose uptake by 44.3 ± 8.8% ($P < .001$, $n = 6$) (Figure 4A). Nesfatin-1 also increased 2-deoxy-D-[^{3}H]glucose uptake by primary cultured neonatal rat cardiomyocytes significantly by 14.8 ± 3.3% at 10 nM ($P < .001$, $n = 8$) and by 23 ± 5.5% at 100 nM ($P <$

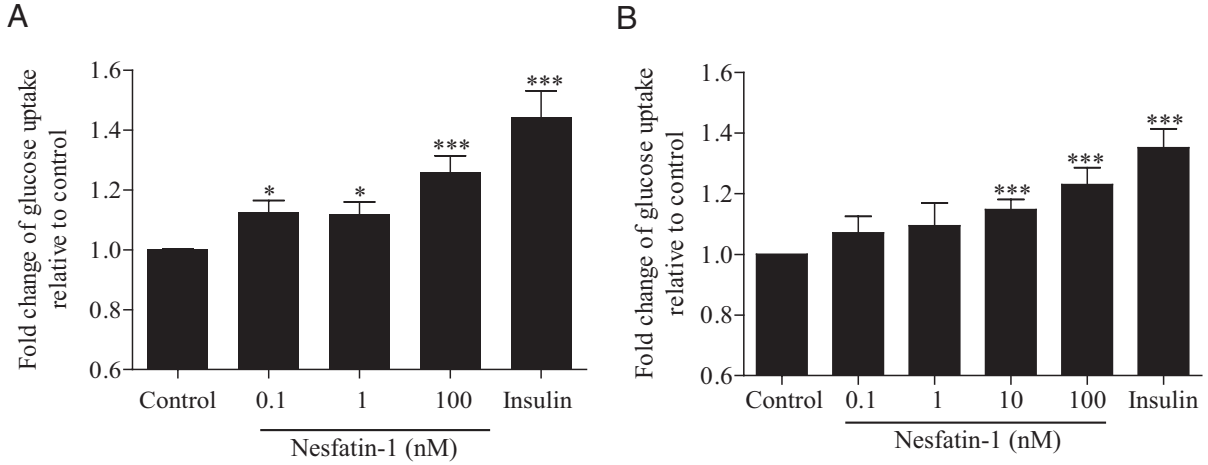

Figure 4. Uptake of 2-deoxy-D-[^{3}H]glucose by HL-1 (A; $n = 11$) and neonatal rat (B; $n = 8$) cardiomyocytes after 2.5 hours of treatment with nesfatin-1 (0.1–100 nM) or 1 hour of treatment with 100 nM insulin, relative to untreated controls. *, $P < .05$; ***, $P < .001$.

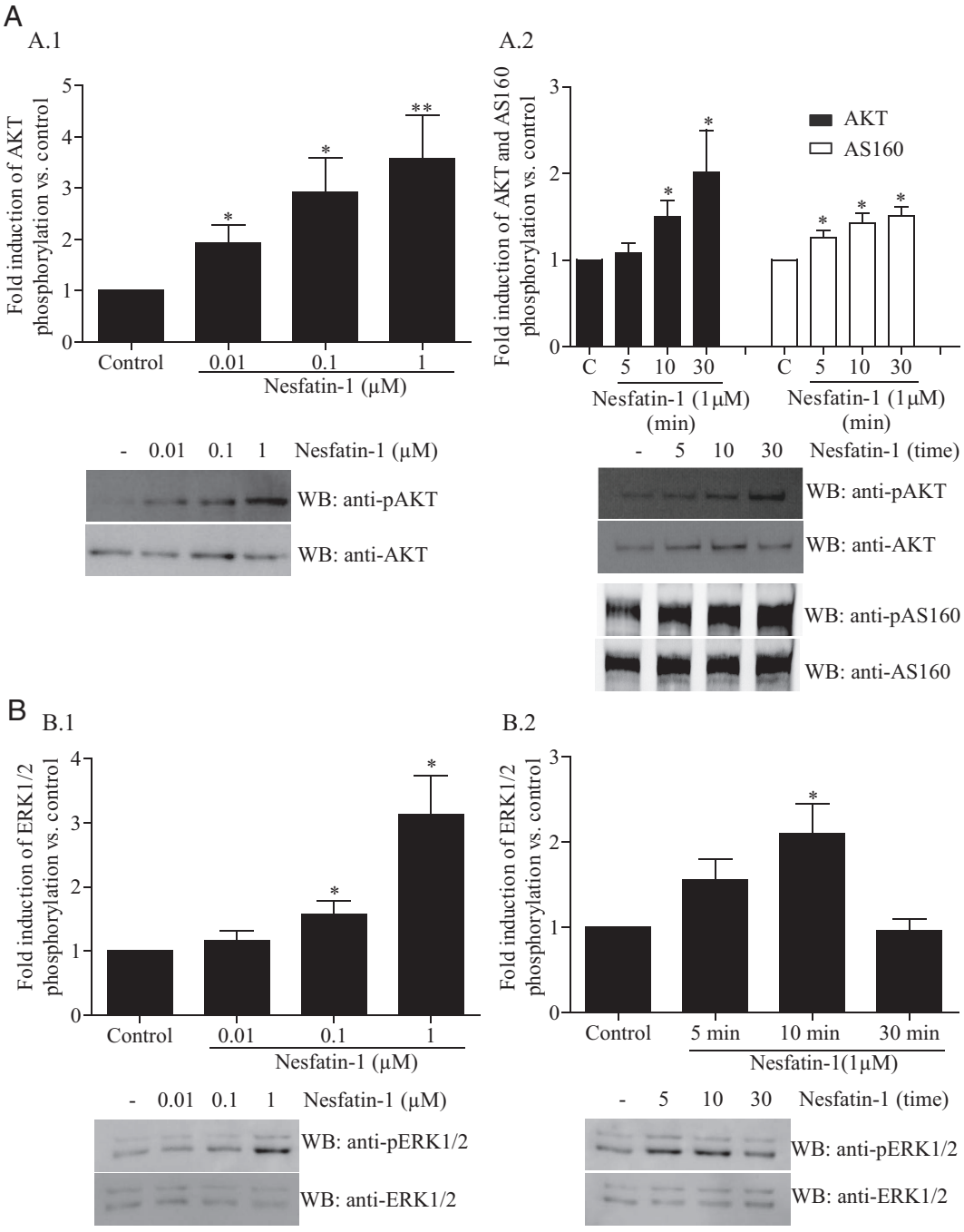

Figure 5. Western blots (WBs) confirmed the activation of AKT, AS160, and ERK1/2 in nesfatin-1-treated neonatal rat cardiomyocytes. A.1, Dependence of AKT phosphorylation on the nesfatin-1 dose ($n = 8$). A.2, Dependence of AKT ($n = 8$) and AS160 ($n = 6$) phosphorylation on treatment duration. B, Dependence of ERK1/2 phosphorylation on nesfatin-1 dose ($n = 7$) and on treatment duration ($n = 6$). *, $P < .05$; **, $P < .01$.

.001, $n = 8$), whereas treatment with 100 nM insulin for 1 hour increased 2-deoxy-D-[^{3}H]glucose uptake by 35.2 ± 6.2% ($P < .001$, $n = 8$) (Figure 4B).

Nesfatin-1 induces AKT, AS160, and ERK1/2 phosphorylation in cardiomyocytes

Because both AKT and ERK1/2 are kinases involved in the stimulation of GLUT-4 translocation and glucose uptake in muscle and cardiac cells (35, 36), we investigated their phosphorylation under nesfatin-1 stimulus in cultured neonatal rat cardiomyocytes. Nesfatin-1 induced dose- and time-dependent increases in the phosphorylation of both AKT and ERK1/2 (Figure 5). In addition, the AKT substrate of 160 kDa (AS160) was also phosphorylated after nesfatin-1 treatments (Figure 5).

Response of rat cardiac nesfatin-1 levels to diet

The high-fat diet increased nesfatin-1 mRNA/protein levels in rat atria but not in ventricular tissue (Figure 6A). Rat atrial NUCB2 mRNA and plasma NUCB2/nesfatin-1 levels were positively correlated with each other and with body fat as a percentage of body weight (Figure 6A.3). Gene expression levels of the predominant cardiac fatty acid transporter CD36 were similar in the hearts of rats fed with the high-fat and standard diets, and we could not find any correlation between CD36 and nesfatin-1 cardiac gene expression levels or between CD36 gene expression and body weight or percentage of body fat (data not shown).

Influences on human cardiac nesfatin-1 levels

In the whole group of patients from whom atrial tissue was obtained, atrial NUCB2 mRNA levels were significantly higher in women without coronary injury (CI) than in those with CI or in men with or without CI (Figure 6B). No other demographic, anthropometric, biochemical, or pharmacological parameters were observed to affect NUCB2 gene expression in cardiac atria.

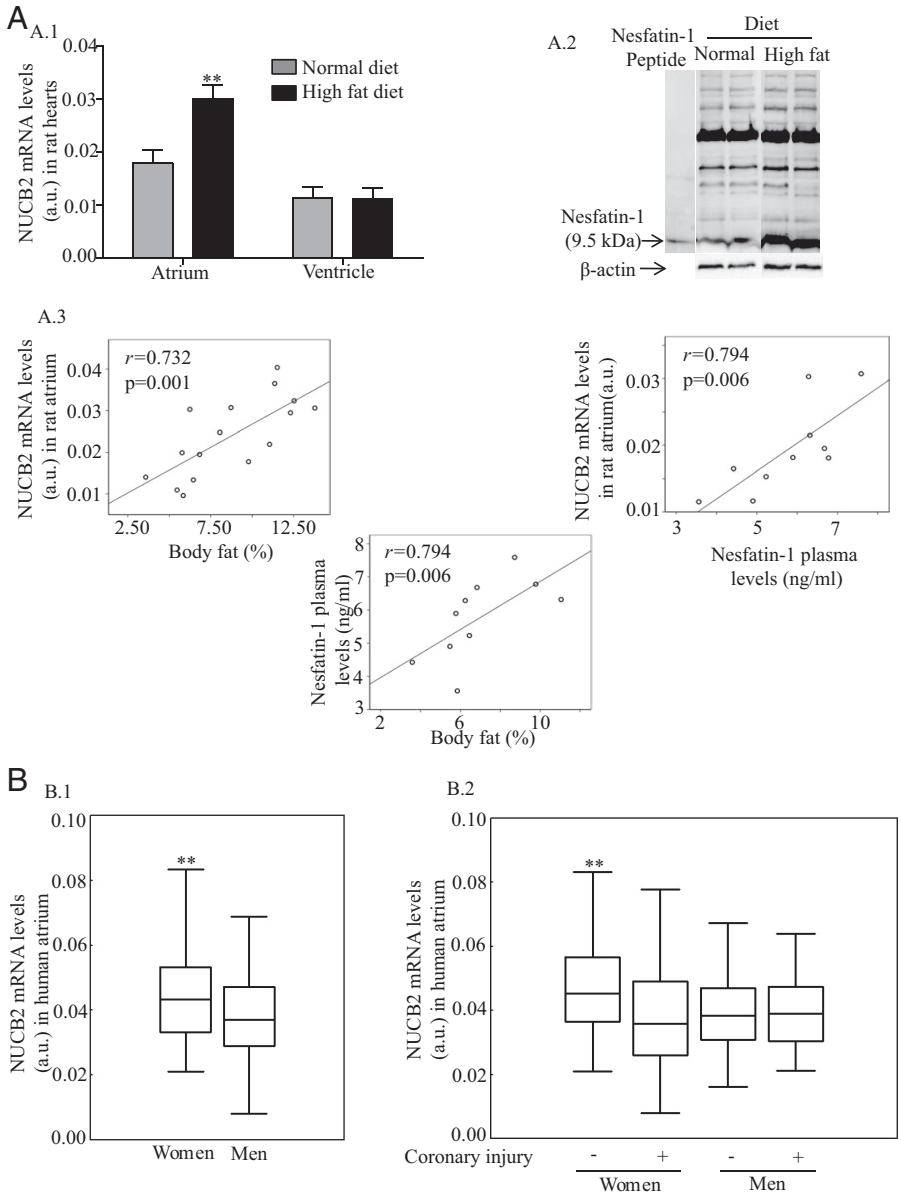

Figure 6. Influence of diet, sex, and coronary injury on cardiac nesfatin-1 levels. A, In rat atrium, the high-fat diet increased NUCB2 gene expression (A.1; $n = 8$) and nesfatin-1 levels (A.2). A.3, Rat atrial NUCB2 mRNA levels correlated positively with body fat as a percentage of body weight ($n = 16$) and plasma nesfatin-1 levels ($n = 10$), which correlated positively to body fat ($n = 10$). B, Atrial NUCB2 mRNA levels (median, [interquartile range]) were higher in women ($n = 90$) than in men ($n = 178$), but lower in women with coronary injury ($n = 27$) than in women without ($n = 62$). **, $P < .01$. a.u., arbitrary units.

Discussion

Adipokines have emerged as the nexus linking obesity, inflammation, metabolic syndrome, and cardiovascular disease (37, 38). The ability of nesfatin-1 to cross the blood-brain barrier suggested the existence of peripheral sources, and expression of its proprotein NUCB2 was later observed in a number of extracerebral tissues (see Introduction). Hitherto there have been two reports of NUCB2 expression in cardiac tissue, both in rats (22, 25), but only Angelone et al (25) detected nesfatin-1 itself, as a band of approximately 9 kDa in Western blots. In fact, this latter study and that of Oh-I et al (1) concerning rat cerebrospinal fluid have been the only occasions on which endogenous fully processed mature nesfatin-1 has unequivocally been observed.

In this work we found that nesfatin-1 is synthesized and secreted by human and murine cardiomyocytes. Western blots showed the 9-kDa nesfatin-1 band in lysates of primary cultures devoid of the other cell types (fibroblasts, endothelial cells, and erythrocytes) that may be present in cardiac tissue extracts. Immunostains showed a clear perinuclear location, very probably in the endoplasmic reticulum or in the Golgi apparatus, both of them typically located all around the nuclear envelope in cardiomyocytes (39, 40). Human atrial tissue was also immunoreactive for prohormone convertase 1/3, the enzyme catalyzing the cleavage of NUCB2 to yield nesfatin-1.

In culture medium of neonatal rat cardiomyocytes, the ELISA-measured NUCB2/nesfatin-1 concentration was in the same range as that detected in the culture medium of adipose tissue explants (6).

Recent reports suggested that nesfatin-1 acts as a multifunctional metabolic hormone. In particular, there is considerable evidence of its being a glucose-dependent coadjuvant of insulin, because it has an antihyperglycemic effect (18) and influences the excitability of glucosensing neurons in rat hypothalamus (20), being able to stimulate glucose-induced insulin release and insulin sensitivity in rats and in mouse islet β-cells (13, 19, 41) and secretion of glucagon from mouse pancreatic islets (17). Moreover, the release of NUCB2/nesfatin-1 from rat pancreatic islets is stimulated by glucose (13), and plasma glucose and NUCB2/nesfatin-1 levels are negatively correlated in rats and in patients with type 2 diabetes (5, 8, 16). However, ours is the first study of its direct effect on GLUT-4 (the main glucose transporter in the heart) translocation. We found that in cultured cardiomyocytes nesfatin-1 alters the distribution of GLUT-4, favoring translocation from the cytoplasmic perinuclear regions to cell peripherals to an extent similar to that induced by insulin, and thus appears to be directly involved in the regulation of cardiomyocyte glucose metabolism. Moreover, our results show that nesfatin-1 induces an increase in glucose uptake by HL-1 mouse cardiac cells and neonatal rat cardiomyocytes in culture. A similar direct effect has been observed previously only in adipocytes from nesfatin-1–treated rats, in which both basal and insulin-induced glucose uptake were significantly increased (13). Note that the concentrations of nesfatin-1 in our experiments, as in several other recent studies of its cellular effects (17, 23, 42, 43), were orders of magnitude higher than the nanomolar concentrations found in human and murine plasma (6, 7, 16), suggesting that in vivo these effects might require a local nesfatin-1 source.

Nesfatin-1 induced dose- and time-dependent increases in the phosphorylation of AKT and ERK1/2, which are both involved in promoting GLUT-4 translocation and glucose uptake in muscle and cardiac cells (35, 36). Our findings parallel observations that central nesfatin-1 administration in rats induces AKT activation in hypothalamic nuclei that mediate glucose homeostasis (19) and that ERK1/2 is activated by nesfatin-1 treatment in perfused rat hearts (25) (although without AKT activation).

In cardiomyocytes, nesfatin-1 promotes the phosphorylation of the AKT substrate AS160, the most distal insulin-signaling protein that has been linked to GLUT-4 translocation (44). Of note, ours are the first results showing that nesfatin-1 can induce the phosphorylation of AS160, and this could indeed help to clarify the physiological/pathophysiological roles of nesfatin-1 in glucose and energy metabolism suggested previously by others (45). Under basal conditions, the Rab GTPase-activating protein domain of AS160 stimulates hydrolysis of Rab-associated GTP and the formation of the inactive GDP-bound Rab, which restrains GLUT-4 exocytosis; however, insulin-stimulated phosphorylation of AS160 by AKT relieves this restraint by leading to an increase in the GTP-bound Rab which, in turn, favors greater GLUT-4 exocytosis to cell surface membranes (44, 46). AS160 is considered to be a point of convergence for coordinating physiological regulation of GLUT-4 membrane recruitment in cardiomyocytes (47).

In rodents, synthesis of nesfatin-1 (or at least NUCB2) appears to respond to diet or nutritional status both centrally in the hypothalamic paraventricular nucleus (1, 48) and in peripheral tissues such as the stomach (49), adipose tissue (6), and heart (this work), where it may help control energy expenditure and may respond to developmental and hormonal signals as well as to metabolic status. The finding that cardiac and plasma NUCB2/nesfatin-1 levels are positively correlated and that both correlate with body fat is in keeping with a report that plasma NUCB2 con-

centrations are higher in mice with diet-induced obesity than in nonobese mice (6).

Obesity imposes a metabolic stress to the heart, which may ultimately lead to cardiac metabolic inflexibility and lipotoxicity, because the fatty acid transporter CD36 is responsible for the chronically increasing uptake of fatty acids by the cardiac muscle under those circumstances (36). In this work, the high-fat diet did not induce changes in cardiac CD36 gene expression, and there was no correlation between cardiac CD36 and nesfatin-1 levels; however, we cannot exclude the possibility that nesfatin-1 could affect the surface presence of CD36 and its translocation from intracellular storage compartments, and future experiments should clarify a possible involvement of this peptide in the complex interplay between signaling pathways and trafficking components known to be involved in the regulation of GLUT-4 and CD36 translocation (36).

Only 2 previous studies have investigated NUCB2/nesfatin-1 regulation in human cells or tissues. Yamada et al (50) found that troglitazone stabilizes NUCB2 mRNA through ERK1/2 activation in a human medulloblastoma cell line, and Riva et al (17) found that NUCB2 deficiency in the pancreatic islets of type 2 diabetes patients can be remedied by culture in glucolipotoxic conditions. In the present study, atrial NUCB2 mRNA levels were significantly higher in women without coronary lesions than in other patients, suggesting a sex-dependent relationship between cardiac nesfatin-1 levels and cardiovascular disease.

In conclusion, nesfatin-1 is synthesized and helps to regulate glucose metabolism in the hearts of humans and experimental animals, where its levels vary with diet and ischemic cardiomyopathy.

Acknowledgments

We thank Patricia Viaño for expert technical assistance.

Address all correspondence and requests for reprints to: Dr Francisca Lago, Laboratorio 7, Instituto de Investigaciones Sanitarias de Santiago de Compostela, Hospital Clínico Universitario, Travesía Choupana s/n, 15706 Santiago de Compostela, Spain. E-mail: francisca.lago.paz@sergas.es.

This work was funded by the Health Research Fund of the Carlos III Health Institute (FIS11/00497) and the Spanish Society of Cardiology. V.G.-R. is funded by the University Professional Development Program (FPU) of the Spanish Ministry of Education, M.F.O. by the Rio Hortega Program of the Spanish Ministry of Economy and Competitiveness, D.R.-P. by the International PhD School, Santiago de Compostela University S.F.-B. and A.M.-L. by the IDICHUS Research Foundation of Santiago de Compostela University Clinical Hospital; and L.M.S., O.G., and F.L. by SERGAS.

Disclosure Summary: The authors have nothing to disclose.

References

1. **Oh-I S, Shimizu H, Satoh T, et al.** Identification of nesfatin-1 as a satiety molecule in the hypothalamus. *Nature*. 2006;443:709–712.
2. **Yosten GL, Samson WK.** The anorexigenic and hypertensive effects of nesfatin-1 are reversed by pretreatment with an oxytocin receptor antagonist. *Am J Physiol Regul Integr Comp Physiol*. 2010;298:R1642–R1647.
3. **García-Galiano D, Navarro VM, Gaytan F, Tena-Sempere M.** Expanding roles of NUCB2/nesfatin-1 in neuroendocrine regulation. *J Mol Endocrinol*. 2010;45:281–290.
4. **Sedbazar U, Maejima Y, Nakata M, Mori M, Yada T.** Paraventricular NUCB2/nesfatin-1 rises in synchrony with feeding suppression during early light phase in rats. *Biochem Biophys Res Commun*. 2013;434:434–438.
5. **Li QC, Wang HY, Chen X, Guan HZ, Jiang ZY.** Fasting plasma levels of nesfatin-1 in patients with type 1 and type 2 diabetes mellitus and the nutrient-related fluctuation of nesfatin-1 level in normal humans. *Regul Pept*. 2010;159:72–77.
6. **Ramanjaneya M, Chen J, Brown JE, et al.** Identification of nesfatin-1 in human and murine adipose tissue: a novel depot-specific adipokine with increased levels in obesity. *Endocrinology*. 2010;151:3169–3180.
7. **Tsuchiya T, Shimizu H, Yamada M, et al.** Fasting concentrations of nesfatin-1 are negatively correlated with body mass index in nonobese males. *Clin Endocrinol (Oxf)*. 2010;73:484–490.
8. **Zhang Z, Li L, Yang M, Liu H, Boden G, Yang G.** Increased plasma levels of nesfatin-1 in patients with newly diagnosed type 2 diabetes mellitus. *Exp Clin Endocrinol Diabetes*. 2012;120:91–95.
9. **Baar O, Akbal E, Köklü S, et al.** A novel appetite peptide, nesfatin-1 in patients with non-alcoholic fatty liver disease. *Scand J Clin Lab Invest*. 2012;72:479–483.
10. **Shimizu H, Oh-I S, Hashimoto K, et al.** Peripheral administration of nesfatin-1 reduces food intake in mice: the leptin-independent mechanism. *Endocrinology*. 2009;150:662–671.
11. **Maejima Y, Sedbazar U, Suyama S, et al.** Nesfatin-1-regulated oxytocinergic signaling in the paraventricular nucleus causes anorexia through a leptin-independent melanocortin pathway. *Cell Metab*. 2009;10:355–365.
12. **Stengel A, Goebel M, Taché Y.** Nesfatin-1: a novel inhibitory regulator of food intake and body weight. *Obes Rev*. 2011;12:261–271.
13. **Gonzalez R, Perry RL, Gao X, et al.** Nutrient responsive nesfatin-1 regulates energy balance and induces glucose-stimulated insulin secretion in rats. *Endocrinology*. 2011;152:3628–3637.
14. **Könczöl K, Pintér O, Ferenczi S, et al.** Nesfatin-1 exerts long-term effect on food intake and body temperature. *Int J Obes (Lond)*. 2012;36:1514–1521.
15. **Miyata S, Yamada N, Kawada T.** Possible involvement of hypothalamic nucleobindin-2 in hyperphagic feeding in Tsumura Suzuki obese diabetes mice. *Biol Pharm Bull*. 2012;35:1784–1793.
16. **Foo KS, Brauner H, Ostenson CG, Broberger C.** Nucleobindin-2/nesfatin in the endocrine pancreas: distribution and relationship to glycaemic state. *J Endocrinol*. 2010;204:255–263.
17. **Riva M, Nitert MD, Voss U, et al.** Nesfatin-1 stimulates glucagon and insulin secretion and beta cell NUCB2 is reduced in human type 2 diabetic subjects. *Cell Tissue Res*. 2011;346:393–405.
18. **Su Y, Zhang J, Tang Y, Bi F, Liu JN.** The novel function of nesfatin-1: anti-hyperglycemia. *Biochem Biophys Res Commun*. 2010;391:1039–1042.

19. **Yang M, Zhang Z, Wang C, et al.** Nesfatin-1 action in the brain increases insulin sensitivity through Akt/AMPK/TORC2 pathway in diet-induced insulin resistance. *Diabetes*. 2012;61:1959–1968.
20. **Chen X, Dong J, Jiang ZY.** Nesfatin-1 influences the excitability of glucosensing neurons in the hypothalamic nuclei and inhibits the food intake. *Regul Pept*. 2012;177:21–26.
21. **Stengel A, Goebel-Stengel M, Jawien J, Kobelt P, Taché Y, Lambrecht NW.** Lipopolysaccharide increases gastric and circulating NUCB2/nesfatin-1 concentrations in rats. *Peptides*. 2011;32:1942–1947.
22. **Stengel A, Goebel M, Yakubov I, et al.** Identification and characterization of nesfatin-1 immunoreactivity in endocrine cell types of the rat gastric oxyntic mucosa. *Endocrinology*. 2009;150:232–238.
23. **García-Galiano D, Pineda R, Ilhan T, et al.** Cellular distribution, regulated expression, and functional role of the anorexigenic peptide, NUCB2/nesfatin-1, in the testis. *Endocrinology*. 2012;153:1959–1971.
24. **Osaki A, Shimizu H, Ishizuka N, Suzuki Y, Mori M, Inoue S.** Enhanced expression of nesfatin/nucleobindin-2 in white adipose tissue of ventromedial hypothalamus-lesioned rats. *Neurosci Lett*. 2012;521:46–51.
25. **Angelone T, Filice E, Pasqua T, et al.** Nesfatin-1 as a novel cardiac peptide: identification, functional characterization, and protection against ischemia/reperfusion injury. *Cell Mol Life Sci*. 2013;70:495–509.
26. **Yosten GL, Samson WK.** Nesfatin-1 exerts cardiovascular actions in brain: possible interaction with the central melanocortin system. *Am J Physiol Regul Integr Comp Physiol*. 2009;297:R330–R336.
27. **Yamawaki H, Takahashi M, Mukohda M, Morita T, Okada M, Hara Y.** A novel adipocytokine, nesfatin-1 modulates peripheral arterial contractility and blood pressure in rats. *Biochem Biophys Res Commun*. 2012;418:676–681.
28. **Mimee A, Smith PM, Ferguson AV.** Nesfatin-1 influences the excitability of neurons in the nucleus of the solitary tract and regulates cardiovascular function. *Am J Physiol Regul Integr Comp Physiol*. 2012;302:R1297–R1304.
29. **García-Rúa V, Otero MF, Lear PV, et al.** Increased expression of fatty-acid and calcium metabolism genes in failing human heart. *PLoS One*. 2012;7:e37505.
30. **González-Juanatey JR, Iglesias MJ, Alcaide C, Piñeiro R, Lago F.** Doxazosin induces apoptosis in cardiomyocytes cultured in vitro by a mechanism that is independent of α_1-adrenergic blockade. *Circulation*. 2003;107:127–131.
31. **Lear PV, Iglesias MJ, Feijóo-Bandín S, et al.** Des-acyl ghrelin has specific binding sites and different metabolic effects from ghrelin in cardiomyocytes. *Endocrinology*. 2010;151:3286–3298.
32. **Slot JW, Garruti G, Martin S, et al.** Glucose transporter (GLUT-4) is targeted to secretory granules in rat atrial cardiomyocytes. *J Cell Biol*. 1997;137:1243–1254.
33. **Lu H, Buchan RJ, Cook SA.** MicroRNA-223 regulates Glut4 expression and cardiomyocyte glucose metabolism. *Cardiovasc Res*. 2010;86:410–420.
34. **Waller AP, George M, Kalyanasundaram A, et al.** GLUT12 functions as a basal and insulin-independent glucose transporter in the heart. *Biochim Biophys Acta*. 2013;1832:121–127.
35. **Pu J, Peng G, Li L, Na H, Liu Y, Liu P.** Palmitic acid acutely stimulates glucose uptake via activation of Akt and ERK1/2 in skeletal muscle cells. *J Lipid Res*. 2011;52:1319–1327.
36. **Steinbusch LK, Schwenk RW, Ouwens DM, Diamant M, Glatz JF, Luiken JJ.** Subcellular trafficking of the substrate transporters GLUT4 and CD36 in cardiomyocytes. *Cell Mol Life Sci*. 2011;68:2525–2538.
37. **Lago F, Dieguez C, Gómez-Reino J, Gualillo O.** Adipokines as emerging mediators of immune response and inflammation. *Nat Clin Pract Rheumatol*. 2007;3:716–724.
38. **Turer AT, Hill JA, Elmquist JK, Scherer PE.** Adipose tissue biology and cardiomyopathy: translational implications. *Circ Res*. 2012;111:1565–1577.
39. **Kronebusch PJ, Singer SJ.** The microtubule-organizing complex and the Golgi apparatus are co-localized around the entire nuclear envelope of interphase cardiac myocytes. *J Cell Sci*. 1987;88:25–34.
40. **McFarland TP, Milstein ML, Cala SE.** Rough endoplasmic reticulum to junctional sarcoplasmic reticulum trafficking of calsequestrin in adult cardiomyocytes. *J Mol Cell Cardiol*. 2010;49:556–564.
41. **Nakata M, Manaka K, Yamamoto S, Mori M, Yada T.** Nesfatin-1 enhances glucose-induced insulin secretion by promoting Ca^{2+} influx through L-type channels in mouse islet β-cells. *Endocr J*. 2011;58:305–313.
42. **Brailoiu GC, Dun SL, Brailoiu E, et al.** Nesfatin-1: distribution and interaction with a G protein-coupled receptor in the rat brain. *Endocrinology*. 2007;148:5088–5094.
43. **Tagaya Y, Osaki A, Miura A, et al.** Secreted nucleobindin-2 inhibits 3T3–L1 adipocyte differentiation. *Protein Pept Lett*. 2012;19:997–1004.
44. **Cartee GD, Wojtaszewski JF.** Role of AKT substrate of 160 kDa in insulin-stimulated and contraction-stimulated glucose transport. *Appl Physiol Nutr Metab*. 2007;32:557–566.
45. **Nakata M, Yada T.** Role of NUBC2/nesfatin-1 in glucose control: diverse functions in islets, adipocytes and brain [published online ahead of print March 25, 2013; DOI: 10.2174/1381612811319006421]. *Curr Pharm Des*.
46. **Bruss MD, Arias EB, Lienhard GE, Cartee GD.** Increased phosphorylation of AKT substrate of 160 kDa (AS160) in rat skeletal muscle in response to insulin or contractile activity. *Diabetes*. 2005;54:41–50.
47. **Samovski D, Su X, Xu Y, Abumrad NA, Stahl PD.** Insulin and AMPK regulate FA translocase/CD36 plasma membrane recruitment in cardiomyocytes via Rab GAP AS160 and Rab8a Rab GTPase. *J Lipid Res*. 2012;53:709–717.
48. **Kohno D, Nakata M, Maejima Y, et al.** Nesfatin-1 neurons in paraventricular and supraoptic nuclei of the rat hypothalamus coexpress oxytocin and vasopressin and are activated by refeeding. *Endocrinology*. 2008;149:1295–1301.
49. **Li Z, Xu G, Li Y, Zhao J, Mulholland MW, Zhang W.** mTOR-dependent modulation of gastric nesfatin-1/NUCB2. *Cell Physiol Biochem*. 2012;29:493–500.
50. **Yamada M, Horiguchi K, Umezawa R, et al.** Troglitazone, a ligand of peroxisome proliferator-activated receptor-γ, stabilizes NUCB2 (nesfatin) mRNA by activating the ERK1/2 pathway: isolation and characterization of the human NUCB2 gene. *Endocrinology*. 2010;151:2494–2503.